ISAC-Enabled Channel-Aware Beam Management in THz Networks with Sensing Errors

Yunchuan Huang*, Gaojie Chen†, Mihai A. Badiu*, and Justin Coon*
* Department of Engineering Science, University of Oxford, Oxford, UK
† School of Flexible Electronics, Sun Yet-sen University, Guangzhou, China
{yunchuan.huang,mihai.badiu,justin.coon}@eng.ox.ac.uk, chengj235@mail.sysu.edu.cn

***Abstract*—This paper investigates the use of Integrated Sensing and Communication (ISAC) to enhance beam management in Terahertz (THz) networks. Following the 5G numerology, the proposed ISAC scheme leverages the synchronization signal block (SSB) for channel condition perception, environmental blockage sensing, and user tracking, which facilitates timely handovers and beam switching based on sensing results. We develop a system-level stochastic geometry framework to account for line-of-sight (LoS) and non-line-of-sight (NLoS) channel conditions, base station (BS) and blocker densities, and sensing accuracy limitations. This framework yields a semi-closed expression for evaluating the average beam misalignment probability in ISAC networks. We demonstrate the performances of both timeout-induced and sensing error-induced misalignment probabilities, respectively. Furthermore, we propose an optimal resource allocation strategy under noisy sensing conditions to minimize beam misalignment probability. Numerical results are provided to validate our analytical results and illustrate the efficacy and robustness of the proposed ISAC beam management scheme compared to conventional networks. This research can offer insight for ISAC network deployments and configurations.**

***Index Terms*—Beam management, integrated sensing and communications (ISAC), stochastic geometry, 5G new radio**

I. Introduction

Future 6G networks are envisioned to provide ultra-high throughputs for a wide range of use cases. In pursuit of larger bandwidth and higher speed, terahertz (THz) radio access technologies are promising enablers in next-generation wireless networks [1]. Due to the propagation characteristics of the THz bands, narrow and highly directional antenna beam patterns are required on both the transmit and receiver sides of wireless links to compensate for path losses [2]. However, while using narrow beams can enhance antenna gain, it also increases the likelihood of beam misalignment because of line-of-sight (LoS) blockage and user mobility [3]. This poses significant challenges for beam management in THz cellular networks.

The development of THz technologies makes the frequency bands of communication gradually coincide with that of radar, giving rise to the design paradigm of integrated sensing and communications (ISAC), which has been recognised as a technical trend in future wireless networks. The ISAC network allows the reuse of both hardware and spectral resources between sensing and communications to achieve higher spectral efficiency and mutual benefits [4].

Using sensing functionality for efficient and timely beam management is a typical application scenario in ISAC [5], [6]. Specifically, sensing can track the location of user equipment (UE) to improve alignment accuracy and reduce training overhead. Pioneering work [7] pointed out that side information derived from radar in infrastructure can be used to adapt the beams of vehicular communication systems. Following that spirit, the authors in [8] proposed a two-stage Kalman filter-based ISAC frame structure for precise and predictive beam tracking. With regard to sensing with 5G standard, the authors in [9] first explored the feasibility of using synchronization signal block (SSB) for wireless sensing. Furthermore, work [10] proposed a network-level ISAC beam management scheme by SSB sensing, in which an ISAC network can predict link blockage and enable proactive beam switches for users. They evaluated network beam alignment performance using stochastic geometry and demonstrated the power of ISAC. However, existing research does not allow for wireless channel conditions and limitations of sensing capability, which can significantly impact the sensing results and beam alignment performances, especially when sensing resources are limited. How can one quantify those impacts on network performance and design the optimal SSB sensing pattern remain a critical issue.

To address the issues above, this paper proposes a more efficient SSB-based beam management for THz networks as well as the optimal sensing resource allocation strategy. The main contributions of this paper include:

1) We propose a comprehensive network architecture for ISAC-enabled beam management that allows perception of channel condition, environmental blockage detection, and user tracking, which can enable timely handovers and smart beam switches to mitigate the beam misalignment issue in THz networks.
2) Using stochastic geometry, our analysis establishes the performances for the timeout beam misalignment probability and sensing error-induced beam misalignment probability, respectively, explaining their impacts on

This material is based upon work supported in part by, the U. S. Army Research Laboratory and the U. S. Army Research Office under contract/grant number W911NF-24-2-0102, and funded in part by Clareondon Fund Scholarships.

ISAC networks.

3) The optimal resource allocation strategy for the sensing pattern is found to minimize the beam misalignment probability under noisy sensing conditions.
4) We demonstrate extensive simulations to validate our analytical results and showcase the efficacy of the proposed ISAC beam management scheme.

To the best of our knowledge, this paper is the first to study the ISAC-enabled beam management scheme while considering physical conditions and sensing accuracy limitations. The importance of this work lies in providing a more realistic and robust framework for evaluating and optimizing ISAC networks.

The remainder of this paper is organized as follows. In Section II, the system model of outdoor THz networks is introduced. Section III presents the proposed ISAC beam management scheme, performance analysis, and optimal sensing pattern design. Section IV provides extensive numerical results. Finally, the conclusions are drawn in Section V.

II. System Model

A. Network Model

As shown in Fig. 1, we consider a large-scale outdoor downlink wireless network with blockers (such as buildings), which can be applied in most cellular scenarios. The nodes are modelled as round dots with radius $r_{\min}$ and follow the homogeneous Poisson point process (PPP) in a 2-dimensional plane, which is a well-developed mathematical framework for network performance analysis. Base stations (BS), mobile terminals (MT), and blockers follow three independent PPPs with intensity λ_B, λ_M and λ_S. The considered system adopts the maximum receive power (MRP) association rule in BS cells, which means that each MT tends to connect to the closest available BS. This rule leads to a Poisson-Voronoi tessellation and forms the cell boundary. Assume that each BS always has an MT to serve and a BS serves one MT during one resource block. We consider a typical MT that moves in a randomly orientated straight line with a speed of v. According to the isotropy and stationarity of PPP, the typical MT can reflect the average behaviours of users in all possible directions, and its receiving performance can represent the average MT performance in the network.

B. Beamforming Model

We approximate the actual antenna as a sectorized pattern, where each sector corresponds to the main lobe of a BS beam. The beam numbers at the BS and MT sides are denoted as n_B, n_M, and the corresponding beamwidths are $\theta_B = 2\pi/n_B, \theta_m = 2\pi/n_M$, respectively.

The movement of MT involves handovers and beam reselections. A handover occurs at a cell boundary, during which the next serving BS has to choose a new beam for the MT. Within the cell, a beam reselection occurs when the MT moves outside the main lobe of the previous beam. To stay connected in the best serving BS beam, the MT should reselect the beam at the intersections between user trajectory and beam boundaries. For the Poisson-Voronoi tessellation, the beam switching points follow the Poisson distribution with intensity of [11]

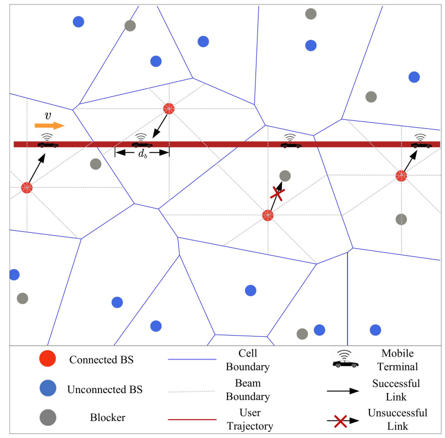

Fig. 1. Network deployment model with a directional beamform.

$$\mu_g = (n_B\sqrt{\lambda_B})/\pi. \tag{1}$$

Therefore, $1/\mu_g$ is the average distance between two consecutive BS's beam boundaries, and the coverage of a single beam d_b follows the exponential distribution with parameter μ_g.

C. Blockage and Channel Model

The presence of blockages dictates whether the channel model between the MT and the BS is LoS or NLoS. In addition to blockers such as buildings (plotted as grey circles in Fig. (1), BSs and MTs are also considered as potential blockers in our work. Considering the molecular absorption and propagation characteristics of THz bands [12], the path loss between MT and BS is expressed as

$$L(r) = \begin{cases} Gr^{-\alpha_L}\exp(-\gamma_L r), & \text{if the link is LoS,} \\ Gr^{-\alpha_N}\exp(-\gamma_N r), & \text{if the link is NLoS.} \end{cases} \tag{2}$$

where G is the constant $\left(\frac{c}{4\pi f_c}\right)^2$ with c the speed of light and f_c the carrier frequency. α_L, α_N are path loss exponents of the LoS and NLoS channel, and γ_L, γ_N are the corresponding absorption coefficients for the LoS and NLoS channels. Usually, $\alpha_L < \alpha_N$,$\gamma_L < \gamma_N$. Let r denote the distance between MT and BS which satisfies $r > 2r_{\min}$ as there is no overlap between each of them.

To evaluate the degradation of signal quality, consider the logarithm of the path loss ratio between LoS and NLoS link β, which is given by

$$\beta \triangleq (\alpha_N - \alpha_L)\ln r + r(\gamma_N - \gamma_L). \tag{3}$$

Since $\alpha_N > \alpha_L, \gamma_N > \gamma_L$, β is a monotonic function of r. In a LoS ball model, given the range threshold $R_T \geq 2r_{\min}$, if $r > R_T$, the corresponding NLoS link is considered not capable of SSB transmission.

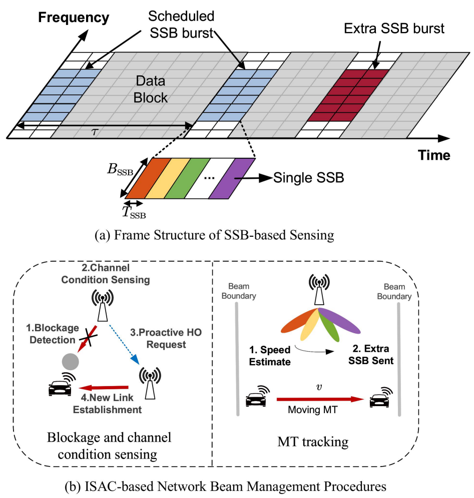

(a) Frame Structure of SSB-based Sensing

(b) ISAC-based Network Beam Management Procedures

Fig. 2. The proposed ISAC-based beam management scheme.

D. Beam Misalignment Challenge

The beam misalignment refers to cases in which the directions of the MT and BS beams are not aligned. As specified by NR [13], the synchronization signal block (SSB) consists of primary synchronization, secondary synchronization, and physical broadcast channel signals. Beam switches are determined by the base stations (BSs) based on beam measurements reported by the users. This requires users to receive at least one SSB burst while remaining within the coverage of the currently connected beam. Accordingly, failure to receive an SSB burst leads to beam misalignment.

In THz networks, either the blockage of the LoS link or the mobility of the MT may cause the interruption of an SSB transmission. Therefore, the misalignment issue can be attributed to the following two cases:

1) **Blockage-induced beam misalignment**: This case happens when the LoS link is blocked by other nodes or blockers, while the NLoS link is considered incapable of reliable SSB transmission.
2) **Mobility-induced beam misalignment**: This case happens when the MT moves too fast to receive scheduled SSB ahead of reaching beam or cell boundaries.

III. ISAC-based Beam Management Scheme

A. System Design

In order to tackle with the beam misalignment issue, the proposed ISAC-based beam management scheme makes use of the omni-directional SSB signal for both environmental blockage sensing and user movement tracking. Following 5G terminology, an SSB burst consisting of a sequence of SSB signals is periodically transmitted over a period τ.

The frame structure of the proposed ISAC network is demonstrated in Fig. 2(a), which follows the 5G NR terminology. Assume that an SSB signal takes up N_s symbols and N_f subcarriers, and that the network has a symbol length T_s and subcarrier spacing Δf. For one SSB, the overall time resource it occupies is $T_{\text{SSB}} = N_s T_s$, and the overall frequency resource is $B_{\text{SSB}} = N_f \Delta f$. The smallest physical transmission resource of the proposed network is the resource element (RE), which occupies one subcarrier in one symbol. Accordingly, the number of RE that one SSB takes up is $N = N_s N_f$. To control the tradeoff between sensing and communications, the resource allocation ratio α is defined as $\alpha \triangleq \ln(N_s)/\ln(N)$, so $N_s = N^{\alpha}, N_f = N^{1-\alpha}$.

The sensing capability in the ISAC network is to track the users and detect potential blockages. As KPIs of sensing, the speed resolution Δv and range resolution Δr rely on how many resources are allocated to SSBs, which can be denoted as [14]

$$\begin{aligned} \Delta v &= c/(2 f_c T_{\text{SSB}}) = c/(2 f_c N^{\alpha} T_s), \\ \Delta r &= c/(2 B_{\text{SSB}}) = c/(2 N^{1-\alpha} \Delta f), \end{aligned} \tag{4}$$

where c is the speed of light, and f_c is centre frequency of the ISAC signal. It should be noted that the relationship between motion resolution Δd_b and the range resolution is

$$\Delta d_b = A_\theta \Delta r = A_\theta \frac{c}{2N^{1-\alpha}\Delta f}, \tag{5}$$

and A_θ is the conversion constant given by:

$$A_\theta \triangleq \frac{\sin\theta_B}{1+\cos\theta_B}(\pi - \theta_B), \tag{6}$$

B. Beam Management Procedures

Compared to [10], which only considers blockage prediction, we propose a more comprehensive beam management scheme that considers both channel condition sensing and MT tracking to keep the beam pair between BS and MT aligned. The beam management of the proposed ISAC network involves the following procedures, as shown in Fig. 2(b):

- **Step 1: Initialization**
  The system begins with the configuration of SSB signal pattern. The initial number of SSBs within an SSB burst is set equal to the beam number n_B. Meanwhile, the SSB period τ, the number of RE N, and the allocation ratio α are specified. Then the first BS builds the link between itself and the MT and starts sensing and data transmission.
- **Step 2: Sensing-aided Beam Switch and Assistance**
  Based on the SSB sensing, the current BS periodically perceives the surroundings for blockage detection, and keeps track of the moving MT to know its kinetic states and location. During this process:
  (1) If the current BS detects potential blockers that could obstruct the LoS link, it will compare the quality of the NLoS channel provided by the current BS with the LoS channel offered by the next closest available BS. Based on this comparison, the BS will decide whether to initiate an inter-cell handover to the next BS or to utilize the NLoS link. Whenever a handover is initiated, the next BS will transmit an extra SSB burst for beam alignment within the *mini-slot* specified in 5G NR [15].
  (2) If the current BS realizes that MT moves too fast, i.e. the estimated speed of MT $\hat{v}$ exceeds the trigger point

$\hat{d}_b/\tau$, it will transmit an additional SSB burst to assist with the intra-cell beam switch.

- **Step 3: Feedback and Adjustment**
  If frequent absence of SSB is reported, BS will increase the number of resource elements N for the better sensing performance.

C. Performance Analysis

We allow for the sensing capability and channel conditions in the analysis of the ISAC network. With sensing functionality, the beam misalignment probability contains two independent parts:

(1) **Handover Timeout:** The blockage-induced handover can introduce additional processing time, which is unacceptable in delay-sensitive THz services. In our setup, a timeout is defined as the event that the links to the nearest K BSs are all blocked. Let $\boldsymbol{P}_{\rm LoS}(r_i)$ denote the LoS probability of a link between MT and $i-$th BS with distance r_i. According to the property of 2D-PPP [16], $\boldsymbol{P}_{\rm LoS}(r_i)$ can be calculated as

$$\boldsymbol{P}_{\rm LoS}(r_i) = e^{-(\lambda_S+\lambda_M)(r_i-2r_{\min})2r_{\min}}, r_i > 2r_{\min}. \tag{7}$$

The timeout event happens when none of the closest K BSs can serve the SSB transmission. So the timeout probability in an ISAC network is

$$\boldsymbol{P}_{\rm to}(\boldsymbol{r}) = \prod_{i=1}^{K}[1-\boldsymbol{P}_{\rm LoS}(r_i)]\mathbb{1}_{\{r_i>R_T\}}. \tag{8}$$

where $\mathbb{1}_{\{.\}}$ is the indicator function. Note that the joint probability density function (pdf) of BS distances $\boldsymbol{r} = \{r_1, r_2, ...r_K\}$ is given by [17]

$$f(\boldsymbol{r}) = e^{-\lambda_{\rm B}\pi(r_K^2-4r_{\min}^2)}(2\lambda_{\rm B}\pi)^K\prod_{i=1}^{K} r_i. \tag{9}$$

Therefore, the average timeout probability with sensing is

$$\begin{aligned} p_{\rm to} &= \mathbb{E}[\boldsymbol{P}_{\rm to}] \\ &= \int\cdots\int_{\mathbf{D}} f(\boldsymbol{r})\prod_{i=1}^{K}[1-\boldsymbol{P}_{\rm LoS}(r_i)]\mathrm{d}r_1...\mathrm{d}r_K, \end{aligned} \tag{10}$$

where integral domain $\mathbf{D} = \{\boldsymbol{r}|R_T < r_1 < r_2 < ... < r_K\}$.

(2) **Sensing error:** Suppose that the sensing capability is sufficient for blockage detection, the beam misalignment occurs when there the speed of MT is underestimated, even though the link quality is good for SSB transmission. This is because the BS misjudges that MT can receive the scheduled SSB burst.

In [10], the estimated value $\hat{v}$ is simply defined as $\hat{v} = v \pm \Delta v$, which overlooks the effect of sensing noise on the estimated speed, leading to inaccuracies under realistic noisy conditions. In this work, we refine this definition by explicitly modeling the effects of noise. Our approach offers a more comprehensive evaluation of sensing accuracy and reliability compared to prior work. Specifically, the speed accuracy and motion accuracy depend on both their respective resolutions and the sensing SNR [18]:

$$\sigma_v^2 = (\frac{\Delta v}{2\pi})^2\frac{6}{N_s\cdot \mathrm{SNR}}, \sigma_{d_b}^2 = \frac{2(\Delta d_b)^2}{\mathrm{SNR}}, \tag{11}$$

where SNR is the signal-to-noise ratio received at the output of a matched filter, and σ_v and σ_{d_b} are the root mean square values (RMS) of the difference between the estimated value of speed and motion and their true values. In the presence of additive white Gaussian noise, the estimated speed $\hat{v}$ and $\hat{d}_b$ at sensing receiver are given by

$$\hat{v} = v + n_v, \hat{d}_b = d_b + n_{d_b}. \tag{12}$$

where $n_v \sim \mathcal{N}(0, \sigma_v^2), n_{d_b} \sim \mathcal{N}(0, \sigma_{d_b}^2)$.

Let $p_{\rm se}$ denote the probability of beam misalignment due to the limited sensing capability. This event occurs when $\hat{v} < \hat{d}_b/\tau$ while actually $v > d_b/\tau$. Therefore

$$\begin{aligned} p_{\rm se} &= \mathbb{P}\left\{v > \frac{d_b}{\tau}, v + n_v < \frac{d_b + n_{d_b}}{\tau}\right\} \\ &= \mathbb{P}\left\{(v+n_v)\tau - n_{d_b} < d_b < v\tau\right\}. \end{aligned} \tag{13}$$

To calculate this probability, first note that d_b follows an exponential distribution with parameter μ_g, and we assume random variables n_v, n_{d_b}, d_b are independent, so $(v+n_v)\tau - n_{d_b} \sim \mathcal{N}(\tau v, \tau^2\sigma_v^2 + \sigma_{d_b}^2) = \mathcal{N}(\mu, \sigma^2)$. Eq. (13) can be computed in a close form

$$\begin{aligned} p_{\rm se} &= \int_{-\infty}^{y}\frac{\exp\left(-\frac{(x-\mu)^2}{2\sigma^2}\right)}{\sqrt{2\pi\sigma^2}}\mathrm{d}x\int_0^{\mu}\mu_g\exp\left(-\mu_g y\right)\mathrm{d}y \\ &= \int_0^{\mu}\frac{1}{2}\left[1+\mathrm{erf}\left(\frac{y-\mu}{\sqrt{2\sigma^2}}\right)\right]\mu_g\exp\left(-\mu_g y\right)\mathrm{d}y \\ &= \frac{1}{2}e^{\left(\frac{\mu_g^2\sigma^2}{2}-\mu\mu_g\right)}\left[\mathrm{erf}\left(\frac{\mu_g\sigma}{\sqrt{2}}\right)-\mathrm{erf}\left(\frac{\mu_g\sigma^2-\mu}{\sqrt{2}\sigma}\right)\right] \\ &\quad -\frac{1}{2}e^{\left(\frac{\mu_g^2\sigma^2}{2}-\mu\mu_g\right)}\mathrm{erf}\left(\frac{\mu}{\sqrt{2}\sigma}\right)+\frac{1}{2}\left(1-e^{-\mu_g\tau v}\right), \end{aligned} \tag{14}$$

where $\mathrm{erf}(\cdot)$ is the error function.

Combining handover timeout and sensing error, the overall beam misalignment probability in the ISAC network is given by

$$p_{\rm mis} = p_{\rm to} + p_{\rm se} - p_{\cap} \overset{(a)}{\approx} p_{\rm to} + p_{\rm se} - p_{\rm to}p_{\rm se}. \tag{15}$$

where $p_{\cap}$ represents the probability of simultaneous timeout and sensing error events. Assuming full blockage detection capability, and leveraging noise / interference mitigation techniques for adaptive MT tracking SNR [19], the timeout and sensing error events can be considered statistically independent, which accounts for the approximation (a).

D. Optimal Resource Allocation Design

Eq. (10) indicates that the timeout probability depends on the density of BS, MT, and blockers and cannot be altered by the sensing patterns. Thus, the beam misalignment probability of the ISAC network depends only on $p_{\rm se}$. According to the

TABLE I
NETWORK PARAMETER SETTINGS

Parameters		Value
$r_{\min}$	Node radius	1 m
f_c	Transmit frequency	1 THz
T_s	Symbol time	4.46 μs
Δf	Subcarrier spacing	240 kHz
τ	SSB burst period	20 ms
K	Max Handover Attempts	2
Sensing SNR		-15 dB
Network deployment	**Suburb**	**Urban**
λ_B BS density	500 km^{-2}	
λ_M MT density	2500 km^{-2}	5000 km^{-2}
v MT speed	60 km/h	40 km/h

second line in (14), $y - \tau v < 0$ in the integral interval $[0, \tau v]$, and the error function is monotonically increasing, so the whole integral is monotonically increasing with the denominator of error function. Therefore, the minimization p_{se} is equivalent to minimizing the value of the variance $\sigma^2 = \tau^2 \sigma_v^2 + \sigma_{d_b}^2$. Substituting (4) into (12), we have

$$\sigma^2(\alpha) = \frac{c^2}{\text{SNR}} \left(\frac{3\tau^2}{8\pi^2 f_c^2 N^{3\alpha} T_s^2} + \frac{A_\theta^2}{2N^{2-2\alpha} \Delta f^2} \right), \quad (16)$$

where we substitute Δv and Δd_b following (4), and $N_s = N^\alpha$. In a specific network, the resource allocation ratio α is flexible. The optimization problem can be formulated as

$$\min_{0<\alpha<1} \sigma^2(\alpha) \Rightarrow \min_{0<\alpha<1} \left\{ \frac{3\tau^2}{8\pi^2 f_c^2 N^{3\alpha} T_s^2} + \frac{A_\theta^2}{2N^{2-2\alpha} \Delta f^2} \right\}. \quad (17)$$

Letting $\frac{d\sigma^2}{d\alpha} = 0$, the optimal α_{opt} is found to be

$$\alpha_{\text{opt}} = \frac{1}{5} \left[\log_N \left(\frac{9\tau^2 \Delta f^2}{8\pi^2 A_\theta^2 f_c^2 T_s^2} \right) + 2 \right]. \quad (18)$$

At THz bands, the center frequency f_c will be much higher than the carrier spacing Δf, leading to $\log_N(\cdot) < 0$. Eq. (18) indicates that α_{opt} increases as the number of sensing resources N increases, which means that the system requires more time-domain resources and fewer frequency-domain resources as N grows.

IV. Numerical Results

This section provides numerical results in different scenarios to show the efficacy of ISAC in mitigating the beam misalignment problem. Specifically, the probability of beam misalignment is compared between the proposed ISAC beam management scheme and conventional networks without sensing. The theoretical model and analysis above are then validated by thorough Monte Carlo simulations. The deployment setups are selected based on 5GAA requirements [20] and 5G NR numerology [21]. Specifically, two different network deployments with different MT density and speeds are considered, reflecting cellular networks in the suburban and urban areas respectively. Assume the MT number $n_M = 1$, and the blocker density λ_S is equal to the MT density λ_M. Detailed system parameters are shown in Table I.

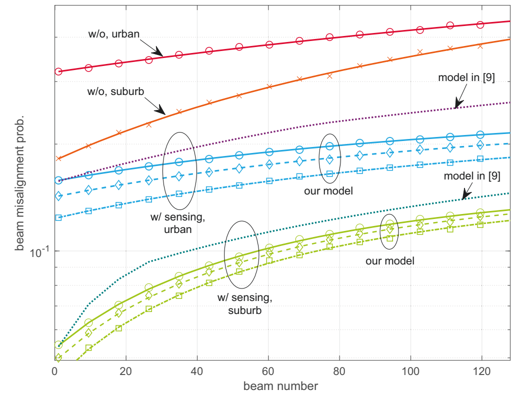

Fig. 3. The beam misalignment probability results in Table I scenarios, where markers are MC simulation results, {circle, diamond, square} correspond to $R_T = \{2, 15, 20\} r_{\min}$, and lines are theory results.

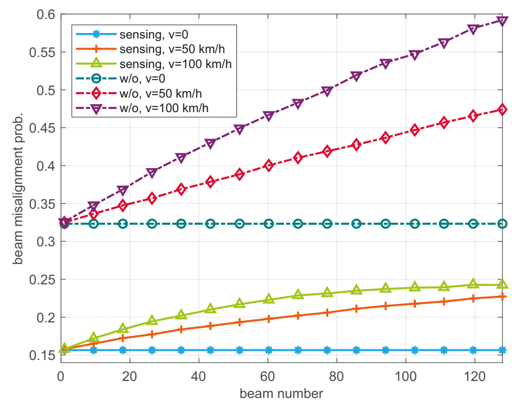

Fig. 4. The beam misalignment probability with different MT speeds.

Fig. 3 compares the beam misalignment performances of the proposed ISAC beam management scheme (labeled w / sensing), conventional networks (labeled w / o), and work [10] with fixed number of resources $N = 4000$. Generally, using more beams causes the increase in beam misalignment probability. The proposed ISAC scheme can significantly mitigate this issue, reducing the beam misalignment probability by approximately 50% across both scenarios examined. Moreover, our model demonstrates superior alignment with simulation data compared to [10], particularly under noisy sensing conditions. Another notable observation is that the misalignment probability decreases when the permitted handover threshold R_T increases. This is because when $R_T = 2r_{\min}$ in the ISAC scheme, we assume that the signal experiences significant path loss, rendering only the LoS link viable. If the link between the MT and the nearest BS is blocked, the MT will always handover to the next closest unblocked. However, if the handover threshold increases to 15 or $20r_{\min}$ and makes use of the NLoS link within the permitted radius range R_T, it can further mitigate the misalignment issue.

Fig. 4 compares the performance with different MT speeds in an urban network deployment. As the MT speed increases, the beam misalignment probability also rises. At higher speeds ($v = 100$ km/h), the misalignment probability for the con-

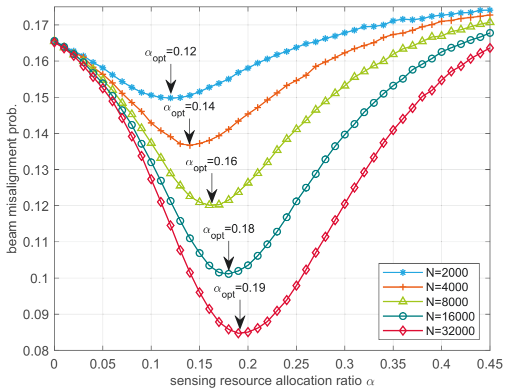

Fig. 5. The beam misalignment probability versus allocation ratio.

ventional network reaches 0.58 when $n_B = 128$, while the ISAC network manages to keep the misalignment probability below 0.25. At lower speeds, the misalignment probability is significantly lower. For the ISAC network, the probability stays around 0.15 when $v = 0$. The results of this figure show that ISAC can effectively address the problem of beam misalignment at higher speeds, demonstrating its robustness under various mobility conditions.

Fig. 5 shows the misalignment probability versus α with different numbers of resources N. The network deployment is suburban. The estimated α^{opt} values, as shown in the figure, closely match the true values that minimize the beam misalignment probability, thereby validating the accuracy of the proposed model and theory. As expected, a larger number of resources leads to better sensing performance and reduced beam misalignment probability. The optimal α also makes a more significant difference when the number of resources is more sufficient. Furthermore, the optimal allocation ratio α_{opt} increases as the number of resources increases. For example, when $N = 2000$, $\alpha_{\text{opt}} = 0.12$, whereas for $N = 32000$, α_{opt} is around 0.19. The results highlight the trade-off between sensing time and frequency resources as well, particularly when the total sensing resources remain fixed.

V. Conclusion

This paper proposed an ISAC-based beam management scheme for THz networks. The proposed scheme uses SSB signals to enable sensing capability for channel perception, blockage detection, and user tracking, which facilitates timely handover and assistance. We analyzed its beam alignment performance under noisy sensing conditions, and presented the optimal design and resource allocation for the sensing pattern. The proposed stochastic geometry framework and simulations demonstrated the power of ISAC over traditional networks, showing that ISAC can significantly reduce beam misalignment for THz systems in different network deployments. Furthermore, we provided insights into trade-offs in sensing time-frequency resource allocation. This work can serve as a foundation for further research into ISAC schemes, especially for next-generation multi-functional wireless networks.

References

[1] Z. Zhang, Y. Xiao, Z. Ma, M. Xiao, Z. Ding, X. Lei, G. K. Karagiannidis, and P. Fan, "6G Wireless Networks: Vision, Requirements, Architecture, and Key Technologies," *IEEE Vehicular Technology Magazine*, vol. 14, no. 3, pp. 28–41, 2019.

[2] D. Moltchanov, E. Sopin, V. Begishev, A. Samuylov, Y. Koucheryavy, and K. Samouylov, "A Tutorial on Mathematical Modeling of 5G/6G Millimeter Wave and Terahertz Cellular Systems," *IEEE Communications Surveys & Tutorials*, vol. 24, no. 2, pp. 1072–1116, 2022.

[3] A. Abusara, H. ElSawy, H. S. Hassanein, A. Noureldin, and A. B. Sediq, "Beam Switching for Intra- and Inter-Cell Mobility in mmWave Networks," in *ICC 2024 - IEEE International Conference on Communications*, pp. 4906–4911, 2024.

[4] F. Liu, Y. Cui, C. Masouros, J. Xu, T. X. Han, Y. C. Eldar, and S. Buzzi, "Integrated Sensing and Communications: Toward Dual-Functional Wireless Networks for 6G and Beyond," *IEEE Journal on Selected Areas in Communications*, vol. 40, no. 6, pp. 1728–1767, 2022.

[5] Q. Xue, C. Ji, S. Ma, J. Guo, Y. Xu, Q. Chen, and W. Zhang, "A survey of beam management for mmWave and THz communications towards 6G," *IEEE Communications Surveys & Tutorials*, 2024.

[6] Y. Nabil, H. ElSawy, S. Al-Dharrab, H. Mostafa, and H. Attia, "Beamwidth Design Tradeoffs in Radar-aided Millimeter-wave Cellular Networks: A Stochastic Geometry Approach," *IEEE Access*, vol. 12, pp. 26196–26211, 2024.

[7] N. González-Prelcic, R. Méndez-Rial, and R. W. Heath, "Radar Aided Beam Alignment in MmWave V2I Communications Supporting Antenna Diversity," in *2016 Information Theory and Applications Workshop (ITA)*, pp. 1–7, 2016.

[8] F. Liu, W. Yuan, C. Masouros, and J. Yuan, "Radar-assisted Predictive Beamforming for Vehicular Links: Communication Served by Sensing," *IEEE Transactions on Wireless Communications*, vol. 19, no. 11, pp. 7704–7719, 2020.

[9] Y. Li, F. Liu, Z. Du, W. Yuan, and C. Masouros, "ISAC-Enabled V2I Networks Based on 5G NR: How Much Can the Overhead Be Reduced?," in *2023 IEEE International Conference on Communications Workshops (ICC Workshops)*, pp. 691–696, 2023.

[10] W. Chen, L. Li, Z. Chen, T. Quek, and S. Li, "Enhancing THz/mmWave Network Beam Alignment with Integrated Sensing and Communication," *IEEE Communications Letters*, vol. 26, no. 7, pp. 1698–1702, 2022.

[11] S. S. Kalamkar, F. Baccelli, F. M. Abinader, A. S. M. Fani, and L. G. U. Garcia, "Beam Management in 5G: A Stochastic Geometry Analysis," *IEEE Transactions on Wireless Communications*, vol. 21, no. 4, pp. 2275–2290, 2022.

[12] N. R. Olson, J. G. Andrews, and R. W. Heath, "Coverage and Capacity of Terahertz Cellular Networks with Joint Transmission," *IEEE Transactions on Wireless Communications*, vol. 21, no. 11, pp. 9865–9878, 2022.

[13] E. Dahlman, S. Parkvall, and J. Skold, *5G NR: The Next Generation Wireless Access Technology*. Academic Press, 2020.

[14] T. Wild, V. Braun, and H. Viswanathan, "Joint Design of Communication and Sensing for Beyond 5G and 6G Systems," *IEEE Access*, vol. 9, pp. 30845–30857, 2021.

[15] V. Loginov, A. Troegubov, A. Lyakhov, and E. Khorov, "Enhanced Collision Resolution Methods with Mini-Slot Support for 5G NR-U," *IEEE Access*, vol. 9, pp. 146137–146152, 2021.

[16] W. Chen, L. Li, Z. Chen, and T. Q. S. Quek, "Coverage Modeling and Analysis for Outdoor THz Networks with Blockage and Molecular Absorption," *IEEE Wireless Communications Letters*, vol. 10, no. 5, pp. 1028–1031, 2021.

[17] D. Moltchanov, "Distance Distributions in Random Networks," *Ad Hoc Networks*, vol. 10, no. 6, pp. 1146–1166, 2012.

[18] M. A. Richards, *Fundamentals of Radar Signal Processing*. McGraw-Hill Education, 2nd ed., 2014.

[19] F. Jin and S. Cao, "Automotive Radar Interference Mitigation Using Adaptive Noise Canceller," *IEEE Transactions on Vehicular Technology*, vol. 68, no. 4, pp. 3747–3754, 2019.

[20] 5GAA Automotive Association, "C-V2X Use Cases Volume II: Examples and Service Level Requirements." White Paper, 2023. 5GAA Automotive Association.

[21] 3GPP, "NR: Physical Layer Procedures for Control," Tech. Rep. 3GPP TS 38.213, 3rd Generation Partnership Project, Mar. 2021.